ACS SENSORS

pubs.acs.org/acssensors

Article

Electrochemical Sensing of Neonicotinoids Using Laser-Induced Graphene

Zachary T. Johnson, Kelli Williams, Bolin Chen, Robert Sheets, Nathan Jared, Jingzhe Li, Emily A. Smith, and Jonathan C. Claussen*

Cite This: *ACS Sens.* 2021, 6, 3063−3071

Read Online

ACCESS | Metrics & More | Article Recommendations | Supporting Information

ABSTRACT: Neonicotinoids are the fastest-growing insecticide accounting for over 25% of the global pesticide market and are capable of controlling a range of pests that damage croplands, home yards/gardens, and golf course greens. However, widespread use has led to nontarget organism decline in pollinators, insects, and birds, while chronic, sublethal effects on humans are still largely unknown. Therefore, there is a need to understand how prevalent neonicotinoids are in the environment as there are currently no commercially available field-deployable sensors capable of measuring neonicotinoid concentrations in surface waters. Herein, we report the first example of a laser-induced graphene (LIG) platform that utilizes electrochemical sensing for neonicotinoid detection. These graphene-based sensors are created through a scalable direct-write laser fabrication process that converts polyimide into LIG, which eliminates the need for chemical synthesis of graphene, ink formulation, masks, stencils, pattern rolls, and postprint annealing commonly associated with other printed graphene sensors. The LIG electrodes were capable of monitoring four major neonicotinoids (CLO, IMD, TMX, and DNT) with low detection limits (CLO, 823 nM; IMD, 384 nM; TMX, 338 nM; and DNT, 682 nM) and a rapid response time (~10 s) using square-wave voltammetry without chemical/biological functionalization. Interference testing exhibited negligible responses from widely used pesticides including the broad-leaf insecticides parathion, paraoxon, and fipronil, as well as systemic herbicides glyphosate (roundup), atrazine, dicamba, and 2,4-dichlorophenoxyacetic acid. These scalable, graphene-based sensors have the potential for wide-scale mapping of neonicotinoids in watersheds and potential use in numerous electrochemical sensor devices.

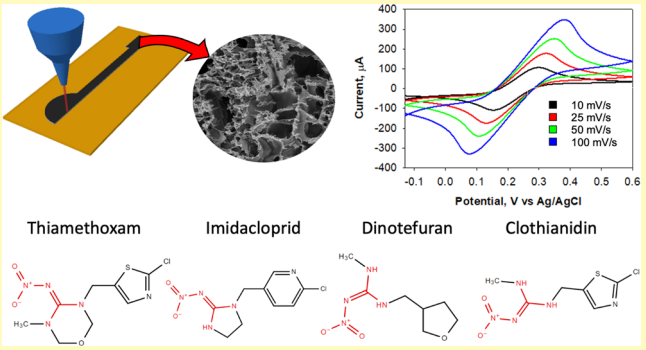

KEYWORDS: *graphene, electrochemical sensor, biosensor, neonicotinoid, pesticide, square-wave voltammetry*

The development of neonicotinoid insecticides over three decades ago is considered a major success in agrochemical research due to their ability to eliminate a broad spectrum of sucking and certain chewing pests that can damage croplands, home yards and gardens, and golf course greens.[1,2] Neonicotinoids exhibit physicochemical advantages over previous generations of pesticides for pest management that have led them to become the fastest-growing insecticide used; neonicotinoids account for over 25% of the global pesticide market.[3,4] Neonicotinoids act within target pests by interfering with the acetylcholine neurotransmitter, ultimately causing neurotoxicity and operate systemically by dispersing throughout a plant system, which consequently causes the plant to become toxic to specific herbivores.[5] Hence, neonicotinoids have negatively impacted a large number of nontarget organisms including a variety of aquatic species[6] and honeybees,[7] primarily due to the significant downregulation of gene expression related to metabolism and detoxification.[8] More specifically, imidacloprid (IMD), thiamethoxam (TMX), clothianidin (CLO), and dinotefuran (DNT) (including their variants S-dinotefuran and *R*-dinotefuran) are the most widely used neonicotinoids and have been shown to be toxic to nontarget species such as honeybees with acute oral LD_{50} ranging from 0.004 to 0.005 μg per bee.[9−11] LD_{50} represents the acute levels that are lethal to 50% of a target population and correspond to exposure time. It has been shown that neonicotinoids negatively impact animals based on moderate-to-high LD_{50} values of neonicotinoids for up to 4 weeks. Furthermore, the LD_{50} value remains moderate to high regardless of the route of exposure in animals.[12] As a result, these neonicotinoids have induced the diminishment of ecosystem biodiversity.[13]

Received: May 25, 2021
Accepted: July 23, 2021
Published: August 9, 2021

The role of neonicotinoids causing human diseases (e.g., cancer) and their long-term effects on ecosystems cannot be conclusively pinpointed due to poor neonicotinoid exposure assessment. Neonicotinoids are becoming more prevalent in a variety of ecosystems, especially in rural agricultural settings. As concentrated neonicotinoids present in seed dressings can drift to neighboring areas during the seed-sowing process, only 1.6−20% of the active neonicotinoid ingredient in the seed dressing is absorbed by the plant, leaving the majority in the soil.[14] Hence, these agrochemicals have percolated into watersheds and drinking waters in the agricultural regions of the Midwestern United States including in private portable wells in the state of Wisconsin at high concentrations (TMX: 1.43 μg/L, IMD: 1.59 μg/L, CLO: 3.88 μg/L).[15] Perhaps, more concerning is a recent study that found neonicotinoids in treated municipal drinking water in the state of Iowa, which suggests that conventional water treatment practices are unable to eliminate neonicotinoids from the water supply.[15,16] Hence, wide-scale knowledge and mapping of neonicotinoid drift, runoff, exposure, and end points are critically important information to help oversee appropriate neonicotinoid stewardship and application methodologies to minimize their environmental impact.

Currently, there are no commercially available in-field sensors available for wide-scale neonicotinoid testing. The standard method for quantifying concentrations of pesticides from field samples requires packaging contaminated samples of soil or water and shipping them to a laboratory for analysis using gas or liquid chromatography coupled with mass spectrometry.[17] These methods are accurate and reproducible for identifying and quantifying analytes but are time-consuming and expensive. They require extensive sample preparation, highly trained personnel, and specialized instrumentation. Inherently, these methods cannot provide real-time or in-field analyte concentrations nor be used to screen large sample sets in a timely and cost-effective manner. Commercially available pesticide field sensors are few and generally consist of colorimetric test strip papers (e.g., pesticide detection test cards by RenekaBio, Agri-Screen, Tickets by Neogen, and OrganaDx by MyDx) that are limited to qualitative (high/negative) outputs and organophosphate and carbamate testing and are easily fouled due to particulate matter found in field samples.[18]

Electrochemical-based biosensors offer a promising solution to monitoring neonicotinoid concentrations in a rapid, quantifiable, low-cost manner that is suitable for large-scale use. Electrochemical sensors are widely researched for in-field sensing as they are not affected by optically dense, turbid fluid that can negatively affect colorimetric sensors and provide an electrical signal that can be directly correlated to analyte concentration levels. Various reports of electrochemical neonicotinoid sensors exist in the literature using a variety of biorecognition agents including molecularly imprinted polymers,[19−21] aptamers,[22−24] antibodies,[25,26] quench bodies, and (Q-bodies),[27] with favorable results for monitoring TMX, IMD, DNT, and/or CLO down to detection limits of 10 ng/mL (IMD) and 4.4 ng/mL (CLO) in garden crop residues and river water. The limitation of these sensors, of course, is that they can only be used once (antibody/aptamer binding to target molecules generally cannot be undone within the context of in-field test conditions), suffer from limited shelf-life due to biorecognition agent degradation, have been limited to typically monitoring just one or two neonicotinoids, and quench body assays can exhibit lower sensitivities than traditional techniques, such as enzyme-linked immunosorbent assays (ELISAs) or high-performance liquid chromatography (HPLC). To create biorecognition element-free neonicotinoid sensors, researchers have used a variety of materials including bismuth, β-cyclodextrin (β-CD), silver, and metal−organic frameworks (MOFs) to directly reduce/oxidize the pesticides to create a measurable electrochemical signal. However, the construction of such sensors is tedious, requiring sputter coating, hydrothermal nanoparticle synthesis, nanoparticle chemical coprecipitation synthesis, magnetic separation, centrifugation, and solvent soaking/rinsing, which elicits the need for a simple, conductive, and direct-write fabrication method that does not require various nanoparticle depositions or metal frameworks.[28−34] Some manuscripts have even attempted to monitor all four of these neonicotinoids, but significant matrix effects and interference from metal cations and surface-active organic compounds were observed.[35] To correct this, a tedious and expensive solid-phase extraction (SPE) procedure was employed, and the level of quantification was only in the microgram range (9−17 μg/L). The referenced work demonstrates the detection of four neonicotinoids: IMD, CLO, DNT, and TMX, without any interference from metal cations; however, it requires expensive and demanding fabrication procedures (e.g., wet thermal oxidation, sputtering).[36] Perhaps some of the more promising results in terms of sensor sensitivity and longevity have come with sensors based on carbon nanomaterials. A variety of carbon-based nanomaterials have been used for neonicotinoid sensing including graphene oxide,[37] nanoparticle-decorated carbon composites,[38] graphene- and graphene oxide-modified glassy carbon electrodes,[28,39,40] multiwalled carbon nanotubes (MWCNTs),[41] and macro−meso−microporous carbon composites.[37] The previously listed sensors have been able to detect neonicotinoids with high selectivity in the micromolar range (e.g., 0.01, 0.1, and 0.04 μM for detection of neonicotinoids in food samples). However, these sensors are not produced in a scalable fashion as they require multiple chemical processing steps including centrifugation, solvent soaks, washing, stirring/mixing, high-temperature pyrolysis (800 °C), heated/fuming acid etching, and electrode polishing to create the carbon nanomaterials and to cast them onto electrode surfaces. Moreover, these sensors are not able to be used continuously or have low shelf-life due to the use of biorecognition agents and/or have not shown to be capable of measuring signals from all four major neonicotinoids, viz., TMX, IMD, DNT, and CLO.

Perhaps one of the more scalable routes to creating carbon nanomaterial-based electrochemical sensors has been with the use of laser-scribed graphene often referred to as laser-induced graphene (LIG).[42−44] LIG is created through a direct-write process that circumvents the need to create graphene/graphene oxide via chemical synthesis (processes that often include high-temperature pyrolysis and/or high-temperature acid etching as used in Hummer's or Brodie method) or create graphene through high-temperature chemical vapor deposition. LIG also eliminates the need for chemical synthesis of graphene and the subsequent ink formulation associated with more scalable printed graphene electrode processes (e.g., screen, gravure, inkjet, and aerosol printing), as well as eliminates the need for masks, stencils, and pattern rolls associated with screen and gravure printing. Moreover, LIG eliminates the need for postprint annealing (e.g., rapid-pulse, thermal, or photonic annealing) that is needed to evaporate ink

https://doi.org/10.1021/acssensors.1c01082
ACS Sens. 2021, 6, 3063−3071

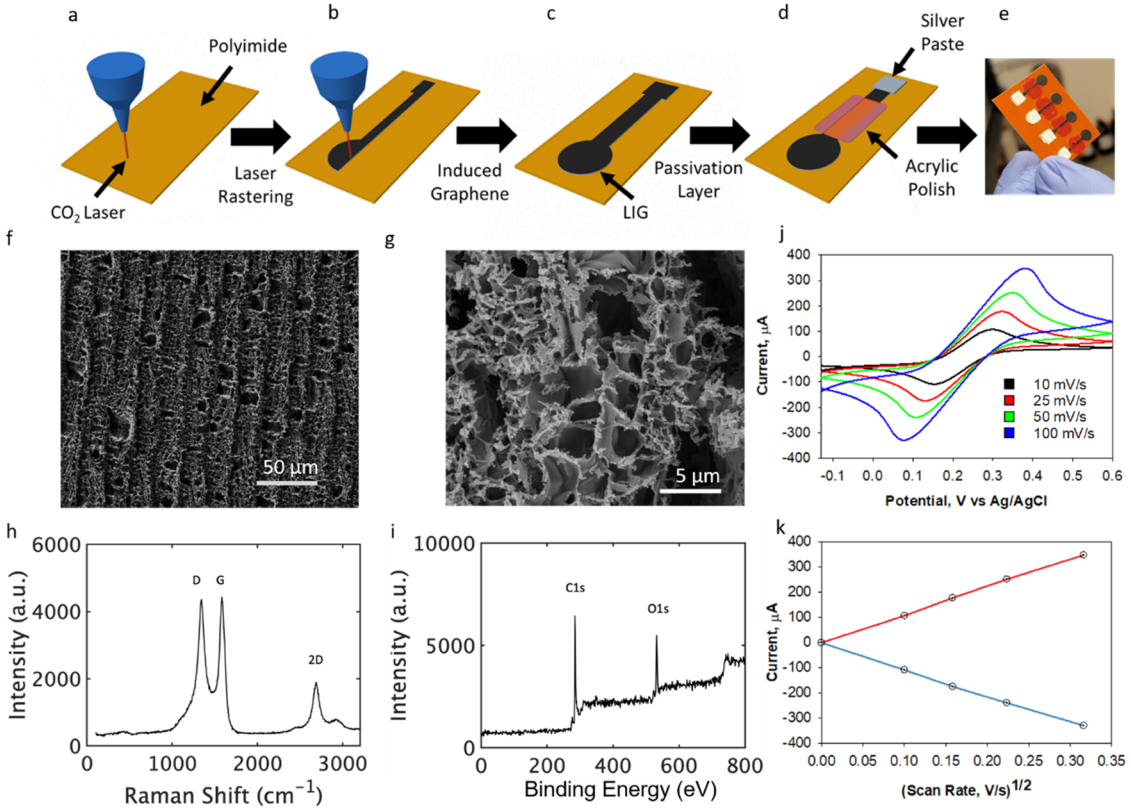

Figure 1. Schematic of the fabrication process: (a) CO_2 laser on bare PI before laser scribing, (b) CO_2 laser scribing, (c) resultant LIG, (d) application of acrylic polish as a passivation layer on the electrode stem and silver paste application on the electrode contact pad, and (e) actual image of LIG. Characterization of the laser-induced graphene electrode: (f) SEM image at 500x magnification, (g) SEM image taken at 5000× magnification, (h) Raman spectrum, (i) XPS survey, (j) cyclic voltammograms at 10, 25, 50, and 100 mV/s in 5 mM ferri/ferrocyanide, and (k) Randles−Sevcik plot.

solvent and carbonize ink binders (e.g., ethyl and nitrocellulose) to make the printed graphene sufficiently conductive for electronic applications such as sensing. Furthermore, the porous and high-defect nature of LIG improves heterogeneous charge transport during electrochemical sensing, which consequently improves target analytes to electrode mass transport/binding, reduces the ohmic reduction in electrical potential, and leads to the ability to measure small currents within low sample volumes.[45] Hence, researchers have used LIG to electrochemically sense a wide variety of target analytes including fertilizer and hydration ions in complex matrices such as in soil and sweat,[46,47] nitrogen compounds and *Salmonella* bacteria in food samples,[48,49] impedance-based cell tracking,[50] aptamer-based biosensing in serum,[51] and bodily metabolites in sweat.[52] To the best of our knowledge, only one example exists of LIG-based pesticide detection.[53] This LIG-based pesticide biosensor used the enzyme organophosphorus hydrolase immobilized on the graphene electrode for the detection of the organophosphate methyl parathion on actual crop surfaces in real time.[53] These results are promising, but the irreversible inhibition of the enzyme does not permit multiple uses, and its shelf-life would be limited to the use of a natural biorecognition element. There does not exist in the research literature, to date, an LIG sensor capable of neonicotinoid monitoring.

Herein, we report the first example of using LIG for neonicotinoid sensing. We demonstrate how the biorecognition element-free LIG electrode can be used to selectively monitor four major neonicotinoids (CLO, IMD, TMX, and DNT) with a rapid response time (~10 s) through the use of square-wave voltammetry (SWV). More specifically, the sensor is capable of monitoring these major neonicotinoids from other pesticides that are commonly used in conjunction with neonicotinoids in the Midwestern United States including other broad-leaf insecticides such as parathion, paraoxon, and fipronil, as well as systemic herbicides glyphosate (roundup), atrazine, dicamba, and 2,4-dichlorophenoxyacetic acid (2,4-D). The reported sensor obtained low detection limits (CLO, 823 nM; IMD, 384; TMX, 338; and DNT 682 nM), which are below the regulatory threshold level (40.05 μM per European Union standards) in freshwater.[54] Finally, neonicotinoid monitoring was confirmed in actual complex biological matrices with river water samples collected from the South Skunk River in the state of Iowa.

RESULTS AND DISCUSSION

LIG Electrode Characterization. The graphene morphology and thickness were characterized by scanning electron microscopy (SEM; Figure 1f,g). The low-magnification (500×) image shows a groove-like morphology along the lasing direction, while the high-magnification (5000×) image shows numerous pores at different scales ranging from 2 to 5 μm. The chemical compositions of the obtained LIG were analyzed by X-ray photoelectron spectroscopy (XPS) (Figure 1i). A strong XPS signal was obtained from the carbon (C) C 1s peak and the oxygen (O) O 1s peak, which resulted in a C/O ratio of 9.1, indicating a high degree of carbonization of the polyimide (PI) after lasing. Raman spectroscopy confirmed the

https://doi.org/10.1021/acssensors.1c01082
ACS Sens. 2021, 6, 3063−3071

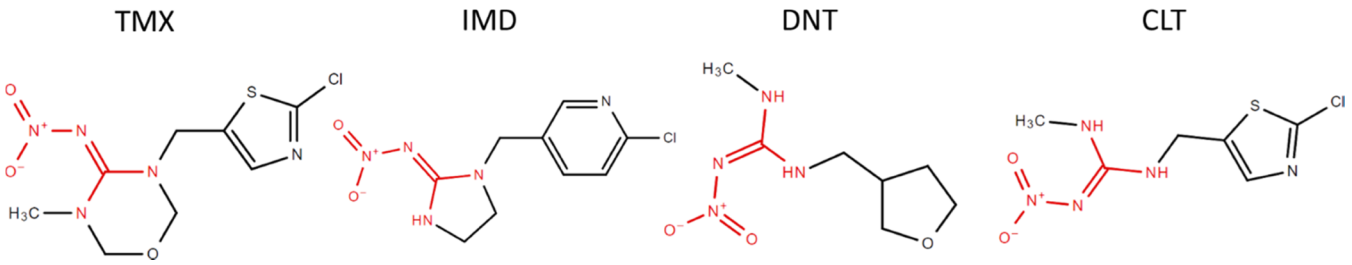

Figure 2. Chemical structure of different neonicotinoids with the nitroguanidine functional group highlighted in red.

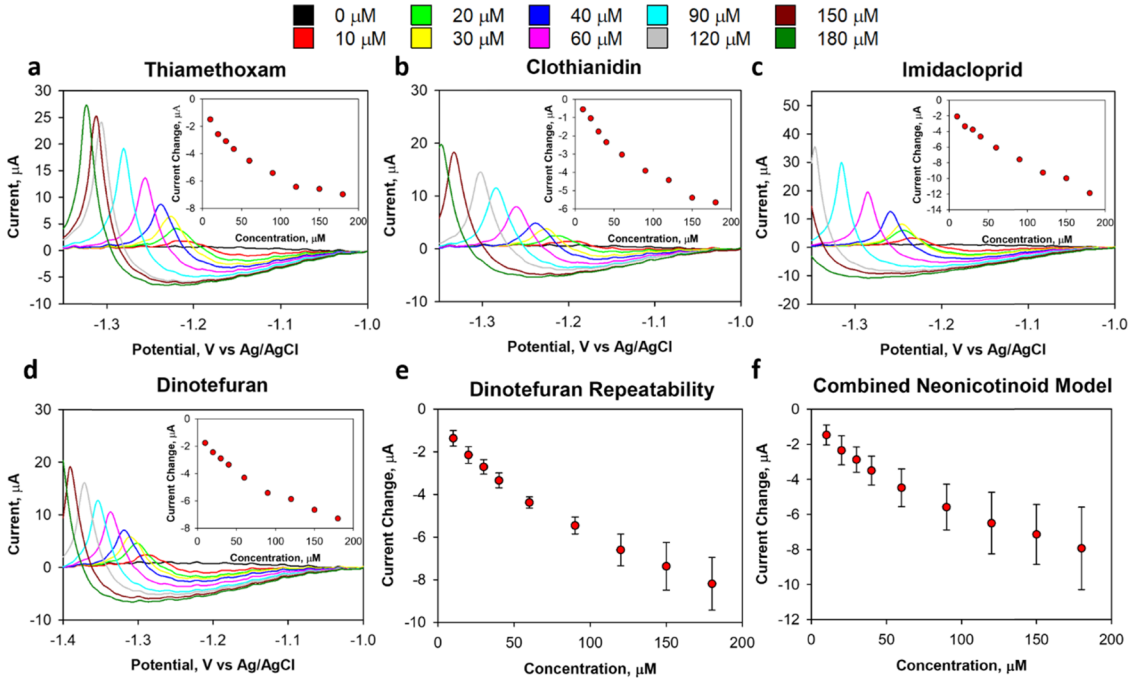

Figure 3. Square-wave voltammogram and inset calibration plots for (a) thiamethoxam (TMX), (b) clothianidin (CLO), (c) imidacloprid (IMD), (d) dinotefuran (DNT), (e) dinotefuran repeatability, and (f) combined neonicotinoid model.

presence of multilayered graphene after laser scribing the PI as the average 2D/G peak intensity ratio of the carbon surface was 0.36 ± 0.02.[55,56] More specifically, the D peak was observed at 1342 cm^{-1}, which is characteristic of defects on the graphene surface. Similarly, the G peak that is characteristic of the sp^2-bonded carbon atoms was observed at 1583 cm^{-1}. Meanwhile, the 2D band that is indicative of double resonance electron−phonon scattering in graphene was observed at 2687 cm^{-1}.[57,58] The electroactive surface area (ESA) was calculated using the Randles−Sevcik equation (eq 1) by recording the anodic and cathodic current peaks at varying scan rates. The equation expresses the oxidation/reduction peak current (ampere) in the following terms: A is the electroactive surface area (cm^2), D is the diffusion coefficient (7.6 ×10^{-6} cm^2/s), n is the number of electrons transferred in the redox probe, ν is the scan rate (V/s), and C is the bulk concentration of the redox species (5 mM)

$$i_p = 2.69 \times 10^5 AD^{1/2} n^{3/2} \nu^{1/2} C \quad (1)$$

The ESA was calculated as 0.313 cm^2, which is 160% of the geometric surface area (0.196 cm^2). An ESA larger than the geometric surface area can be attributed to the porous, three-dimensional (3D) structure of the graphene, which allows for greater accessibility to the redox solution and electrochemical interactions.[51,59,60] Additionally, the peak current versus the square root of the scan rate behaves linearly (Figure 1j,k). However, the ΔE_p (148−300 mV) indicates a quasireversible system regarding electron transfer, which can be attributed to defects on the LIG.[48,61,62] Additionally, surface morphology was considered as laser parameters can be varied to alter the surface of LIG. Laser settings of 15% speed and 7% power were used to induce hydrophilic LIG, which is necessary for neonicotinoid detection as hydrophilic LIG has been shown to improve the flow and dispersion of aqueous solution at the liquid−solid interface of the electrode.[63] Comparatively, hydrophobic LIG would otherwise repel aqueous solution, thus limiting the reduction of neonicotinoids. Furthermore, settings of 7% speed and 7% power can be used to induce hydrophilic LIG but suffer from limited throughput and time efficiency compared to a speed of 15%.

Electrochemical Sensing of Neonicotinoids. LIG electrodes were calibrated for increasing concentrations of TMX, DNT, IMD, and CLO using square-wave voltammetry (SWV). It should be noted here that SWV is a particular type of differential pulse voltammetry that applies potential in a stepwise manner while recording the anodic or cathodic current associated with the target molecule redox potentials. SWV holds an advantage over cyclic voltammetry and linear sweep voltammetry as SWV amplifies faradic current and

https://doi.org/10.1021/acssensors.1c01082
ACS Sens. 2021, 6, 3063−3071

mitigates noise from capacitive current[64] while performing faster scan rates than differential pulse voltammetry.[65] Hence, SWV is often more accurate than other voltammetry techniques and is used herein to monitor neonicotinoid concentrations in water samples as neonicotinoids have well-established electroactive behavior.

Neonicotinoids are well suited for electrochemical detection because they possess a nitro group that is reduced to a hydroxylamine group, occurring near −1.00 V vs Hg hanging drop electrode.[66] Neonicotinoid peaks on average occurred within a potential window of −1.18 to −1.24 V, thus making it difficult to distinguish different neonicotinoids when combined in the same solution but enabled the selective detection of neonicotinoids against other insecticides and other classes of pesticides such as herbicides. This is attributed to the reduction of the same nitroguanidine group present in all of the neonicotinoids. The chemical structures and the nitroguanidine groups vital for the reduction signal are shown in Figure 2.

The current reduction peaks increased with increasing concentrations of neonicotinoids (Figure 3a−d) from concentrations between 10 and 180 μM. Calibration repeats were performed n = 5 times for DNT, with an average relative standard deviation of 13%, highlighting the reproducibility among multiple sensors (Figure 3e). Sensor stability was tested over time by performing 10 response tests to 40 μM TMX for one sensor (Figure S1). The first test yielded the largest response (2.1 μA) compared to the rest of the tests (1.0−1.1 μA). These responses highlight the stability of the sensor over multiple runs. We hypothesize that the drop in sensitivity after the first test is due to the initial surface fouling as the hydrophilic, highly porous LIG absorbs nonelectroactive species from the solution. The SWV plots for the reduction of each neonicotinoid possessed a sharp anodic peak notable at more negative potentials. We hypothesize that the existence of the observed anodic peak is due to the protonation of reduction products that may formulate rapidly after the reduction of nitroguanidine. The complex reduction of the nitroguanidine group of neonicotinoid pesticides provides challenges due to various protonation states[67] and possible adduct formation of nitroso and hydroxylamine groups present on related aromatic species.[68] The reduction of nitroguanidine has been characterized as a 4-electron reduction to nitrosoguanidine followed by a 2-electron reduction to aminoguanidine. Both reductions are pH-dependent; however, the second reduction is presumably more influenceable because the protonation state determines the rate-limiting step of the reduction.[69] This contributes to a nonlinear relationship between the reduction potentials and pH,[70] which was observed at a pH between 6 and 8 and therefore relates to our described neonicotinoid detection as this is done in phosphate-buffered saline (PBS) at pH 7.4. We postulate that the anodic peak is the result of the newly formed aminoguanidine groups protonating following its production as the pK_b of the species traverses the pH of the buffer. Though the anodic peak shows a greater current response than the cathodic peak, using the anodic response as a means of neonicotinoid detection is unreliable over a pH range of 5.4−9.4 compared to calibrated data at a pH of 7.4 (Figure S2). By observing the response to 40 μM of CLO over various pH points, it is evident that the anodic current response varies more over this pH range than the cathodic current does when compared to the calibrated model at a pH of 7.4 (see Table S1). Overall, the sensor displayed a linear range of 10−40 μM and a detection limit of 823, 384, 338, and 682 nM for CLO, IMD, TMX, and DNT, respectively. The detection limits were considerably lower than the detection limits (8.3 and 7.9 μM for TMX and IMD, respectively) reported that also used SWV.[40] We posit that the lower detection limits are due to the high-surface-area structure of the porous LIG compared to that of the glassy carbon electrode, which provides more locations for electrochemical reduction events.

Next, the electrode response to all four neonicotinoids introduced simultaneously in the same test beaker was monitored. To this end, an overall neonicotinoid calibration was modeled to predict the concentration of a combined neonicotinoid solution (Figure 3f). This was done by averaging the calibration plots of each neonicotinoid due to their similar responses. A 40 μM solution of neonicotinoids (10 μM each of TMX, DNT, CLO, IMD) was tested to confirm the recovery percentage of this model (Table 1). On average, this model predicted a concentration of 42.4 μM showing a 106% recovery. These results indicated that the four neonicotinoids are reduced similarly because of the nitroguanidine group and can be modeled in combination.

Table 1. Combined Neonicotinoid Found Concentration for 40 μM Spike

sensor 1 (μM)	sensor 2 (μM)	sensor 3 (μM)	sensor 4 (μM)	average (μM)	recovery (%)
42.5	36.1	48.2	42.8	42.4	106

Furthermore, the neonicotinoid reduction potentials were compared with potential interference species. These pesticides include the common herbicides atrazine, glyphosate, dicamba, and 2,4-D, as well as common insecticides fipronil, parathion, and paraoxon (Figure 4). Square-wave voltammograms were recorded for 40 μM concentrations of each pesticide. None of the potential interference pesticides showed considerable current change within a neonicotinoid reduction potential window of −1.18 to −1.24 V. The chosen herbicide species atrazine, glyphosate, dicamba, and 2,4-dichlorophenoxyacetic acid have become some of the most prevalent herbicides applied in the Midwest and pose threats of aerosolization and watershed contamination.[71,72] Additionally, the insecticides parathion and paraoxon were investigated as both have shown electroactive behavior between 0 and −0.4 V vs Ag/AgCl,[73−75] a potential window that is inconsequential to the neonicotinoid sensing regime. Neonicotinoid studies to date have not reported a comprehensive pesticide interferent species analysis, as shown in Figure 4.[66,69,76]

Finally, recovery tests were performed in water from the South Skunk River in the state of Iowa. The water was filtered through a 0.45 μm filter, brought to 0.5 M NaCl, and spiked with 40 μM of a neonicotinoid. For comparison, neonicotinoids were detected in deionized water that was also brought to 0.5 M NaCl. The recovery percentages are presented in Table 2 and were calculated using the river water recording as the found response and the deionized water recording as the standard response. The responses shown are the average responses (n = 3) for each pesticide in each fluid. River water recovery tests confirm that a biorecognition element-free sensor can detect neonicotinoids in complex fluids with recoveries of 91.8−108.5%.

https://doi.org/10.1021/acssensors.1c01082
ACS Sens. 2021, 6, 3063−3071

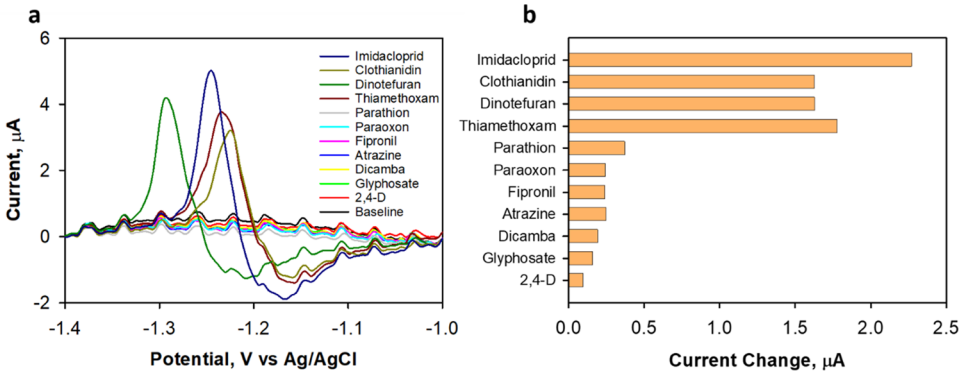

Figure 4. Interference data including (a) square-wave voltammograms and (b) current change comparison using 40 μM concentrations of each pesticide measured against a phosphate-buffered saline baseline without pesticides.

Table 2. River Water Recovery Test

neonicotinoid	DI (μA)	river water (μA)	recovery (%)
clothianidin	9.38	8.60	91.8
imidacloprid	9.16	9.24	100.9
thiamethoxam	7.22	7.83	108.5
dinotefuran	1.77	1.67	94.4

CONCLUSIONS

In conclusion, this work demonstrates one of the first studies to electrochemically determine a family of pesticides, specifically the presence of neonicotinoids, without the use of a biorecognition agent. The reported sensor showcases the first use of biorecognition element-free LIG as a viable platform for the rapid detection of neonicotinoids and demonstrates a more scalable route to multilayered graphene electrodes than more conventional fabrication methods that use low-throughput CVD or chemical/mechanical exfoliation of graphite for graphene synthesis and methods that use screen, gravure, aerosol, or inkjet printing to form the electrode by printing graphene inks obtained from liquid-phase exfoliation of graphite. The lack of a biorecognition agent allows for decreased sensor fabrication and operation complexity and eliminates the need for stringent storage protocols and inherently greatly increases the sensor lifetime. Additionally, the detection of neonicotinoids was not affected by other common herbicides and insecticides, thus bolstering the reported platform as highly selective. The sensor detected neonicotinoid concentrations in complex media such as river water, with recoveries of 91.8, 100.9, 108.5, and 94.4% for CLO, IMD, TMX, and DNT, respectively. The sensor showed a linear range of 10−40 μM and detection limits of 823, 384, 338, and 682 nM for clothianidin, imidacloprid, thiamethoxam, and dinotefuran, respectively.

The broader implications of this work could be significant for those working in monitoring or mapping pesticides across entire watersheds/ecosystems, as well as for those seeking to improve the electrochemical electrode technology in general. The reported sensor circumvents the need to transport river water and soil samples to a lab for chromatographic analysis and allows for on-site testing. Hence, this technology could permit rapid testing of agricultural runoffs and river water and help policy-makers set guidelines on when and where such pesticides can be used. Furthermore, the creation of LIG electrochemical electrodes could be useful for a wide variety of applications that require high surface area and defect-rich graphene for heterogeneous charge transport such as with energy storage elements including supercapacitors,[77,78] batteries,[79] pseudocapacitors,[80] or lithium-ion batteries,[80] as well as multiplex sweat analytes[81] and virus (e.g., SARS-CoV-2) sensors.[82]

EXPERIMENTAL SECTION

LIG Electrode Fabrication and Characterization. The LIG was fabricated by preparing the polyimide (PI) substrate, positioning the laser, laser rastering, which converts sp^3-carbon atoms in PI to sp^2-carbon atoms found in graphene, and the application of acrylic polish and silver ink (Figure 1a−e). The PI substrate is first washed with isopropyl alcohol, and the laser is positioned over the PI with a 2 mm defocus. Laser rastering settings are as follows: 7% power, 15% speed, and 50% frequency. These parameters were used to induce a 5 mm diameter dipstick design. Following the creation of the LIG, acrylic polish was added to prevent wicking and maintain a constant working area on the electrode. Silver ink was added to the contact to prevent abrasion from the potentiostat clips. Scanning electron microscopy images were taken by an FEI Quanta 250 FEG scanning electron microscope using a 10 kV accelerating voltage. The Raman spectrum was collected by a Horiba XploRA Plus confocal Raman microscope. A 532 nm laser with 1.2 mW and a 50× objective with a 0.5 numerical aperture were used to check the sample with a 30 s acquisition and three accumulations. The sample was checked at six random locations, and the average 2D/G peak intensity ratio was calculated from fitting the Raman peaks to the Lorentzian function in Igor Pro 6.37.

Materials and Methods. *Reagents.* Phosphate-buffered saline 10 mM potassium chloride pH 7.4, clothianidin, imidacloprid, thiamethoxam, dinotefuran, atrazine, glyphosate, 2,4-dichlorophenoxyacetic acid, dicamba, paraoxon, parathion, and fipronil were purchased from Sigma-Aldrich. All pesticides were prepared in deionized water (18.4 MΩ cm) except imidacloprid, clothianidin, and fipronil, which were prepared in acetone and 100 times diluted in deionized water. Kapton polyimide film (125 μm) was purchased from DuPont.

Preparation of LIG. A 75 W CO_2 Epilog Fusion M2 Laser was used to convert PI into graphene. A 5 mm diameter working electrode was lased using 15% speed (271.9 mm/s), 7% power (5.25 W), 1200 dots per inch, and a 2 mm defocus length. The contacts were covered with silver paste to mitigate wear on the sensor. Acrylic polish was used as a passivation layer to control the working electrode surface area.

Electrochemical Analysis. Palmsens4 potentiostat was used for all electrochemical measurements. SWV was performed in a 5 mL volume of PBS pH 7.4 in ambient conditions so as to mimic the conditions that a field-deployable sensor is subjected to. The potential was run from −0.6 to −1.5 V with a potential step of 5 mV, an amplitude of 25 mV, and a frequency of 25 Hz. A three-electrode setup was used: LIG working electrode, commercial Ag/AgCl reference electrode, and commercial platinum wire counter electrode. SWV was run 10 times in bare buffer to purge the buffer and electrode

https://doi.org/10.1021/acssensors.1c01082
ACS Sens. 2021, 6, 3063−3071

surface of any redox species that was electroactive in the potential window. Sensors were calibrated to each pesticide by then mixing the pesticide for 2 min at 300 rpm. Stirring was then turned off, and the scan was performed. Sensors were washed 2 times with deionized water before each addition of pesticide. Sensors were disposed of after use. Interference pesticides were tested at 40 μM. Results were reported as a change in current from the initially recorded baseline without the presence of pesticides. The combined neonicotinoid model was calibrated to the average responses of each neonicotinoid for the corresponding concentrations. The validity of the model was tested by mixing 10 μM each of thiamethoxam, dinotefuran, clothianidin, and imidacloprid. This served as a model for 40 μM of neonicotinoid solution. Additionally, sensors were tested in a solution of river water brought to 0.5 M NaCl. A recovery percentage was reported for 40 μM concentration spikes compared to the current response found in 0.5 M NaCl deionized water, which was used as the standard. Data was normalized using the moving average baseline option in the PSTrace program.

■ ASSOCIATED CONTENT

Supporting Information

The Supporting Information is available free of charge at https://pubs.acs.org/doi/10.1021/acssensors.1c01082.

Additional experimental details and methods regarding pH dependence of the cathodic and anodic peak currents and longevity studies (PDF)

■ AUTHOR INFORMATION

Corresponding Author

Jonathan C. Claussen − *Department of Mechanical Engineering, Iowa State University of Science and Technology, Ames, Iowa 50010, United States;* orcid.org/0000-0001-7065-1077; Email: jcclauss@iastate.edu

Authors

Zachary T. Johnson − *Department of Mechanical Engineering, Iowa State University of Science and Technology, Ames, Iowa 50010, United States*

Kelli Williams − *Department of Mechanical Engineering, Iowa State University of Science and Technology, Ames, Iowa 50010, United States*

Bolin Chen − *Department of Mechanical Engineering, Iowa State University of Science and Technology, Ames, Iowa 50010, United States*

Robert Sheets − *Department of Mechanical Engineering, Iowa State University of Science and Technology, Ames, Iowa 50010, United States*

Nathan Jared − *Department of Mechanical Engineering, Iowa State University of Science and Technology, Ames, Iowa 50010, United States*

Jingzhe Li − *Department of Chemistry, Iowa State University, Ames, Iowa 50011, United States; The Ames Laboratory, U.S. Department of Energy, Ames, Iowa 50011, United States;* orcid.org/0000-0002-1856-1477

Emily A. Smith − *Department of Chemistry, Iowa State University, Ames, Iowa 50011, United States; The Ames Laboratory, U.S. Department of Energy, Ames, Iowa 50011, United States;* orcid.org/0000-0001-7438-7808

Complete contact information is available at: https://pubs.acs.org/10.1021/acssensors.1c01082

Notes

The authors declare no competing financial interest.

■ ACKNOWLEDGMENTS

J.C.C. gratefully acknowledges funding support for this work by the National Science Foundation under award numbers ECCS-1841649 and CMMI-2037026, as well as from the National Institute of Food and Agriculture, U.S. Department of Agriculture, under award number 2016-67021-25038, 2021-67021-34457, and 2021-67011-35130.

■ REFERENCES

(1) Jeschke, P.; Nauen, R. Neonicotinoids—from Zero to Hero in Insecticide Chemistry. *Pest Manage. Sci.* **2008**, *1098*, 1084−1098.

(2) Bonner, M. R.; Alavanja, M. C. R. Pesticides, Human Health, and Food Security. *Food Energy Secur.* **2017**, *6*, 89−93.

(3) Simon-Delso, N.; Amaral-Rogers, V.; Belzunces, L. P.; Bonmatin, J. M.; Chagnon, M.; Downs, C.; Furlan, L.; Gibbons, D. W.; Giorio, C.; Girolami, V.; et al. Systemic Insecticides (Neonicotinoids and Fipronil): Trends, Uses, Mode of Action and Metabolites. *Environ. Sci. Pollut. Res.* **2015**, *22*, 5−34.

(4) Craddock, H. A.; Huang, D.; Turner, P. C.; Quirós-alcalá, L.; Payne-sturges, D. C. Trends in Neonicotinoid Pesticide Residues in Food and Water in the United States, 1999−2015. *Environ. Health* **2019**, *18*, No. 7.

(5) Gibbons, D.; Morrissey, C.; Mineau, P. A Review of the Direct and Indirect Effects of Neonicotinoids and Fipronil on Vertebrate Wildlife. *Environ. Sci. Pollut. Res.* **2015**, *22*, 103−118.

(6) Morrissey, C. A.; Mineau, P.; Devries, J. H.; Sanchez-Bayo, F.; Liess, M.; Cavallaro, M. C.; Liber, K. Neonicotinoid Contamination of Global Surface Waters and Associated Risk to Aquatic Invertebrates: A Review. *Environ. Int.* **2015**, 291−303.

(7) Bonmatin, J. M.; Giorio, C.; Girolami, V.; Goulson, D.; Kreutzweiser, D. P.; Krupke, C.; Liess, M.; Long, E.; Marzaro, M.; Mitchell, E. A.; et al. Environmental Fate and Exposure; Neonicotinoids and Fipronil. *Environ. Sci. Pollut. Res.* **2015**, *22*, 35−67.

(8) Christen, V.; Schirrmann, M.; Frey, J. E.; Fent, K. Global Transcriptomic Effects of Environmentally Relevant Concentrations of the Neonicotinoids Clothianidin, Imidacloprid, and Thiamethoxam in the Brain of Honey Bees (Apis Mellifera). *Environ. Sci. Technol.* **2018**, *52*, 7534−7544.

(9) Gregorc, A.; Alburaki, M.; Rinderer, N.; Sampson, B.; Knight, P. R.; Karim, S.; Adamczyk, J. Effects of Coumaphos and Imidacloprid on Honey Bee (Hymenoptera: Apidae) Lifespan and Antioxidant Gene Regulations in Laboratory Experiments. *Sci. Rep.* **2018**, *8*, No. 15003.

(10) Decio, P.; Ustaoglu, P.; Roat, T. C.; Malaspina, O.; Devaud, J. M.; Stöger, R.; Soller, M. Acute Thiamethoxam Toxicity in Honeybees Is Not Enhanced by Common Fungicide and Herbicide and Lacks Stress-Induced Changes in MRNA Splicing. *Sci. Rep.* **2019**, *9*, No. 19196.

(11) Chen, Z.; Yao, X.; Dong, F.; Duan, H.; Shao, X.; Chen, X.; Yang, T.; Wang, G.; Zheng, Y. Ecological Toxicity Reduction of Dinotefuran to Honeybee: New Perspective from an Enantiomeric Level. *Environ. Int.* **2019**, *130*, No. 104854.

(12) Thompson, D. A.; Lehmler, H. J.; Kolpin, D. W.; Hladik, M. L.; Vargo, J. D.; Schilling, K. E.; Lefevre, G. H.; Peeples, T. L.; Poch, M. C.; Laduca, L. E.; et al. A Critical Review on the Potential Impacts of Neonicotinoid Insecticide Use: Current Knowledge of Environmental Fate, Toxicity, and Implications for Human Health. *Environ. Sci.: Processes Impacts* **2020**, *22*, 1315−1346.

(13) Van Der Sluijs, J. P.; Amaral-Rogers, V.; Belzunces, L. P.; Bijleveld Van Lexmond, M. F.; Bonmatin, J. M.; Chagnon, M.; Downs, C. A.; Furlan, L.; Gibbons, D. W.; Giorio, C.; et al. Conclusions of the Worldwide Integrated Assessment on the Risks of Neonicotinoids and Fipronil to Biodiversity and Ecosystem Functioning. *Environ. Sci. Pollut. Res.* **2015**, *22*, 148−154.

(14) Wood, T. J.; Goulson, D.; Wood, T. J. The Environmental Risks of Neonicotinoid Pesticides: A Review of the Evidence Post 2013. *Environ. Sci. Pollut. Res.* **2017**, *24*, 17285−17325.

(15) Id, B. Z. B.; Huseth, A. S.; Id, R. L. G. Widespread Detections of Neonicotinoid Contaminants in Central Wisconsin Groundwater. *PLoS One* **2018**, *13*, No. e0201753.
(16) Klarich, K. L.; Nicholas, C. P.; Dewald, E. M.; Hladik, M. L.; Kolpin, D. W.; Cwiertny, D. M.; Lefevre, G. H. Occurrence of Neonicotinoid Insecticides in Finished Drinking Water and Fate during Drinking Water Treatment. *Environ. Sci. Technol. Lett.* **2017**, *4*, 168−173.
(17) Claussen, J. *Mapping the off-Target Effects of Multi-Class Pesticide Contamination through Insect Exposure with Infield Graphene-Based Biosensors and Open Microfluidics*; USDA-NIFA, 2021; Vol. *1387*, pp 1−25.
(18) Claussen, J. *FMRG: Manufacturing Advanced Electronics through Printing Using Bio-Based and Locally Identifiable Compounds (MADE-PUBLIC)*; NSF, 2021; pp 1−34.
(19) Li, S.; Liu, C.; Yin, G.; Luo, J.; Zhang, Z. Supramolecular Imprinted Electrochemical Sensor for the Neonicotinoid Insecticide Imidacloprid Based on Double Amplification by Pt-In Catalytic Nanoparticles and a Bromophenol Blue Doped Molecularly Imprinted Film. *Microchim. Acta* **2016**, 3101−3109.
(20) Zhang, W.; Liu, C.; Han, K.; Wei, X.; Xu, Y.; Zou, X.; Zhang, H. Biosensors and Bioelectronics A Signal On-off Ratiometric Electrochemical Sensor Coupled with a Molecular Imprinted Polymer for Selective and Stable Determination of Imidacloprid. *Biosens. Bioelectron.* **2020**, *154*, No. 112091.
(21) Kong, L.; Jiang, X.; Zeng, Y.; Zhou, T.; Shi, G. Sensors and Actuators B: Chemical Molecularly Imprinted Sensor Based on Electropolmerized Poly (o-Phenylenediamine) Membranes at Reduced Graphene Oxide Modified Electrode for Imidacloprid Determination. *Sens. Actuators, B* **2013**, *185*, 424−431.
(22) Taghdisi, S. M.; Danesh, N. M.; Ramezani, M. Electrochemical Aptamer Based Assay for the Neonicotinoid Insecticide Acetamiprid Based on the Use of an Unmodified Gold Electrode. *Microchim. Acta* **2017**, 499−505.
(23) Yang, L.; Sun, H.; Wang, X.; Yao, W.; Zhang, W.; Jiang, L. An Aptamer Based Aggregation Assay for the Neonicotinoid Insecticide Acetamiprid Using Fluorescent Upconversion Nanoparticles and DNA Functionalized Gold Nanoparticles. *Microchim. Acta* **2019**, *186*, No. 308.
(24) Bahreyni, A.; Yazdian-robati, R.; Ramezani, M.; Abnous, K. Fluorometric aptasensing of the neonicotinoid insecticide acetamiprid by using multiple complementary strands and gold nanoparticles. *Microchim. Acta* **2018**, *185*, No. 272.
(25) Reynoso, E. C.; Torres, E.; Bettazzi, F.; Palchetti, I. Trends and Perspectives in Immunosensors for Determination of Currently-Used Pesticides: The Case of Glyphosate, Organophosphates, and Neonicotinoids. *Biosensors* **2019**, *9*, No. 20.
(26) Uchigashima, M.; Watanabe, E.; Ito, S.; Iwasa, S.; Miyake, S.; Division, D.; Technology, A. S. Development of Immunoassay Based on Monoclonal Antibody Reacted with the Neonicotinoid Insecticides Clothianidin and Dinotefuran. *Sensors* **2012**, *12*, 15858−15872.
(27) Zhao, S.; Dong, J.; Jeong, H.; Okumura, K.; Ueda, H. Rapid Detection of the Neonicotinoid Insecticide Imidacloprid Using a Quenchbody Assay. *Anal. Bioanal. Chem.* **2018**, *410*, 4219−4226.
(28) Liu, G.; Li, L.; Xu, D.; Huang, X.; Xu, X.; Zheng, S.; Zhang, Y.; Lin, H. Metal − Organic Framework Preparation Using Magnetic Graphene Oxide-Cyclodextrin for Neonicotinoid Pesticide Adsorption and Removal. *Carbohydr. Polym.* **2017**, *175*, 584−591.
(29) Bhardwaj, R.; Rao, R. P.; Mukherjee, I.; Kumar, P. Layered Construction of Nano Immuno-Hybrid Embedded MOF as an Electrochemical Sensor for Rapid Quanti Fi Cation of Total Pesticides Load in Vegetable Extract. *J. Electroanal. Chem.* **2020**, *873*, No. 114386.
(30) El-akaad, S.; Mohamed, M. A.; Elmasri, M. M.; Abdelwahab, N. S.; Abdelaleem, E. A.; Saeger, S.; De; Beloglazova, N. 3D bismuth ferrite microflowers electrochemical sensor for the multiple detection of pesticides. *J. Electrochem. Soc.* **2020**, *167*, No. 027543.
(31) Papp, Z.; Vajdle, O. Bismuth Modified Carbon-Based Electrodes for the Determination of Selected Neonicotinoid Insecticides. *Molecules* **2011**, *16*, 4451−4466.
(32) Elisa, A.; Oliveira, F.; Bettio, G. B.; Ce, A. Optimization of an Electrochemical Sensor for Determination of Imidacloprid Based on b -Cyclodextrin Electropolymerization on Glassy Carbon Electrode. *Electroanalysis* **2018**, *30*, 1929−1937.
(33) Ajermoun, N.; Farahi, A.; Lahrich, S.; Bakasse, M.; Saqrane, S.; Abderrahim, M.; Mhammedi, E. Electrocatalytic activity of the metallic silver electrode for thiamethoxam reduction: application for the detection of a neonicotinoid in tomato and orange samples. *J. Sci. Food Agric.* **2019**, *99*, 4407−4413.
(34) Ajermoun, N.; Aghris, S.; Farahi, A.; Lahrich, S.; Saqrane, S.; Bakasse, M.; El Mhammedi, M. A. Electrochemical Reduction of Neonicotinoids Insecticides Catalysed by Metallic Silver: Case of the Detection of Imidacloprid in Tomato and Orange Juices. *Int. J. Environ. Anal. Chem.* **2021**, *101*, 585−597.
(35) Lezi, N.; Economou, A. Voltammetric Determination of Neonicotinoid Pesticides at Disposable Screen-Printed Sensors Featuring a Sputtered Bismuth Electrode. *Electroanalysis* **2015**, *27*, 2313−2321.
(36) Lezi, N.; Economou, A. Voltammetric Determination of Neonicotinoid Pesticides at Disposable Screen-Printed Sensors Featuring a Sputtered Bismuth Electrode. *Electroanalysis* **2015**, *27*, 2313−2321.
(37) Wang, Q.; Zhangsun, H.; Zhao, Y.; Zhuang, Y.; Xu, Z.; Bu, T.; Li, R.; Wang, L. Macro-Meso-Microporous Carbon Composite Derived from Hydrophilic Metal-Organic Framework as High-Performance Electrochemical Sensor for Neonicotinoid Determination. *J. Hazard. Mater.* **2021**, *411*, No. 125122.
(38) Ganesamurthi, J.; Keerthi, M.; Chen, S.-M.; Shanmugam, R. Electrochemical Detection of Thiamethoxam in Food Samples Based on Co3O4 Nanoparticle@Graphitic Carbon Nitride Composite. *Ecotoxicol. Environ. Saf.* **2020**, *189*, No. 110035.
(39) Xie, T.; Zhang, M.; Chen, P.; Zhao, H.; Yang, X. A Facile Molecularly Imprinted Electrochemical Sensor Based on Graphene: Application to the Selective Determination of Thiamethoxam in Grain. *RSC Adv.* **2017**, *7*, 38884−38894.
(40) Urbanová, V.; Bakandritsos, A.; Jakubec, P.; Szambó, T.; Zbořil, R. A Facile Graphene Oxide Based Sensor for Electrochemical Detection of Neonicotinoids. *Biosens. Bioelectron.* **2017**, *89*, 532−537.
(41) Bruzaca, E. E. S.; De Oliveira, R. C.; Duarte, M. S. S.; Sousa, C. P.; Morais, S.; Correia, A. N.; De Lima-Neto, P. Electrochemical Sensor Based on Multi-Walled Carbon Nanotubes for Imidacloprid Determination. *Anal. Methods* **2021**, *13*, 2124−2136.
(42) Ye, R.; James, D. K.; Tour, J. M. Laser-Induced Graphene. *Acc. Chem. Res.* **2018**, *51*, 1609−1620.
(43) Duy, L. X.; Peng, Z.; Li, Y.; Zhang, J.; Ji, Y.; Tour, J. M. Laser-Induced Graphene Fibers. *Carbon* **2018**, *126*, 472−479.
(44) Chyan, Y.; Ye, R.; Li, Y.; Singh, S. P.; Arnusch, C. J.; Tour, J. M. Laser-Induced Graphene by Multiple Lasing: Toward Electronics on Cloth, Paper, and Food. *ACS Nano* **2018**, *12*, 2176−2183.
(45) Marques, A. C.; Cardoso, A. R.; Martins, R.; Sales, M. G. F.; Fortunato, E. Laser-Induced Graphene-Based Platforms for Dual Biorecognition of Molecules. *ACS Appl. Nano Mater.* **2020**, *3*, 2795−2803.
(46) Garland, N. T.; McLamore, E. S.; Cavallaro, N. D.; Mendivelso-Perez, D.; Smith, E. A.; Jing, D.; Claussen, J. C. Flexible Laser-Induced Graphene for Nitrogen Sensing in Soil. *ACS Appl. Mater. Interfaces* **2018**, *10*, 39124−39133.
(47) An, Q.; Gan, S.; Xu, J.; Bao, Y.; Wu, T.; Kong, H.; Zhong, L.; Ma, Y.; Song, Z.; Niu, L. A Multichannel Electrochemical All-Solid-State Wearable Potentiometric Sensor for Real-Time Sweat Ion Monitoring. *Electrochem. Commun.* **2019**, *107*, No. 106553.
(48) Soares, R. R. A.; Hjort, R. G.; Pola, C. C.; Parate, K.; Reis, E. L.; Soares, N. F. F.; McLamore, E. S.; Claussen, J. C.; Gomes, C. L. Laser-Induced Graphene Electrochemical Immunosensors for Rapid and Label-Free Monitoring of *Salmonella enterica* in Chicken Broth. *ACS Sens.* **2020**, *5*, 1900−1911.

https://doi.org/10.1021/acssensors.1c01082
ACS Sens. 2021, 6, 3063−3071

(49) Vanegas, D.; Patiño, L.; Mendez, C.; Oliveira, D.; Torres, A.; Gomes, C.; McLamore, E. Laser Scribed Graphene Biosensor for Detection of Biogenic Amines in Food Samples Using Locally Sourced Materials. *Biosensors* **2018**, *8*, No. 42.
(50) Puetz, P.; Behrent, A.; Baeumner, A.; Wegener, J. Laser-Scribed Graphene (LSG) as New Electrode Material for Impedance-Based Cellular Assays. *Sens. Actuators, B* **2020**, *321*, No. 128443.
(51) Fenzl, C.; Nayak, P.; Hirsch, T.; Wolfbeis, O. S.; Alshareef, H. N.; Baeumner, A. J. Laser-Scribed Graphene Electrodes for Aptamer-Based Biosensing. *ACS Sens.* **2017**, *2*, 616−620.
(52) Yang, Y.; Song, Y.; Bo, X.; Min, J.; Pak, O. S.; Zhu, L.; Wang, M.; Tu, J.; Kogan, A.; Zhang, H.; et al. A Laser-Engraved Wearable Sensor for Sensitive Detection of Uric Acid and Tyrosine in Sweat. *Nat. Biotechnol.* **2020**, *38*, 217−224.
(53) Zhao, F.; He, J.; Li, X.; Bai, Y.; Ying, Y.; Ping, J. Smart Plant-Wearable Biosensor for in-Situ Pesticide Analysis. *Biosens. Bioelectron.* **2020**, *170*, No. 112636.
(54) Wolfram, J.; Stehle, S.; Bub, S.; Petschick, L. L.; Schulz, R. Meta-Analysis of Insecticides in United States Surface Waters: Status and Future Implications. *Environ. Sci. Technol.* **2018**, *52*, 14452−14460.
(55) Wang, Q. H.; Jin, Z.; Kim, K. K.; Hilmer, A. J.; Paulus, G. L. C.; Shih, C. J.; Ham, M. H.; Sanchez-Yamagishi, J. D.; Watanabe, K.; Taniguchi, T.; et al. Understanding and Controlling the Substrate Effect on Graphene Electron-Transfer Chemistry via Reactivity Imprint Lithography. *Nat. Chem.* **2012**, *4*, 724−732.
(56) Nguyen, V. T.; Le, H. D.; Nguyen, V. C.; Ngo, T. T. T.; Le, D. Q.; Nguyen, X. N.; Phan, N. M. Synthesis of Multi-Layer Graphene Films on Copper Tape by Atmospheric Pressure Chemical Vapor Deposition Method. *Adv. Nat. Sci. Nanosci. Nanotechnol.* **2013**, *4*, No. 035012.
(57) Tehrani, F.; Bavarian, B. Facile and Scalable Disposable Sensor Based on Laser Engraved Graphene for Electrochemical Detection of Glucose. *Sci. Rep.* **2016**, *6*, No. 27975.
(58) Pimenta, M. A.; Dresselhaus, G.; Dresselhaus, M. S.; Cançado, L. G.; Jorio, A.; Saito, R. Studying Disorder in Graphite-Based Systems by Raman Spectroscopy. *Phys. Chem. Chem. Phys.* **2007**, 1276−1291.
(59) Nayak, P.; Kurra, N.; Xia, C.; Alshareef, H. N. Highly Efficient Laser Scribed Graphene Electrodes for On-Chip Electrochemical Sensing Applications. *Adv. Electron. Mater.* **2016**, *2*, No. 1600185.
(60) Griffiths, K.; Dale, C.; Hedley, J.; Kowal, M. D.; Kaner, R. B.; Keegan, N. Laser-Scribed Graphene Presents an Opportunity to Print a New Generation of Disposable Electrochemical Sensors. *Nanoscale* **2014**, *6*, 13613−13622.
(61) Aristov, N.; Habekost, A. Cyclic Voltammetry-A Versatile Electrochemical Method Investigating Electron Transfer Processes. *World J. Chem. Educ.* **2015**, *3*, 115−119.
(62) Nayak, P.; Kurra, N.; Xia, C.; Alshareef, H. N. Highly Efficient Laser Scribed Graphene Electrodes for On-Chip Electrochemical Sensing Applications. *Adv. Electron. Mater.* **2016**, *2*, No. 1600185.
(63) Nasser, J.; Lin, J.; Zhang, L.; Sodano, H. A. Laser Induced Graphene Printing of Spatially Controlled Super-Hydrophobic/Hydrophilic Surfaces. *Carbon* **2020**, *162*, 570−578.
(64) Square Wave Voltammetry—an overview|ScienceDirect Topics. https://www.sciencedirect.com/topics/chemistry/square-wave-voltammetry (accessed Jan 14, 2021).
(65) Osteryoung, J. G.; Osteryoung, R. A. Square Wave Voltammetry. *Anal. Chem.* **1985**, *57*, 101−110.
(66) Öndeş, B.; Muti, M. Electrochemical Determination of Neonicotinoid Insecticide Clothianidin by Nanomaterial based Disposable Electrode. *Anal. Bioanal. Electrochem.* **2020**, *12*, 392−401.
(67) Gaál, F. F.; Guzsvány, V. J.; Bjelica, L. J. Determination of Various Insecticides and Pharmaceuticals Using Differently Modified Glassy Carbon Electrodes. *J. Serb. Chem. Soc.* **2007**, *72*, 1465−1475.
(68) Zuman, P.; Fijalek, Z.; Dumanovic, D.; Sužnjević, D. Polarographic and Electrochemical Studies of Some Aromatic and Heterocyclic Nitro Compounds, Part I: General Mechanistic Aspects. *Electroanalysis* **1992**, *4*, 783−794.
(69) Guzsvány, V.; Kádár, M.; Gaál, F.; Tóth, K.; Bjelica, L. Rapid Differential Pulse Polarographic Determination of Thiamethoxam in Commercial Formulations and Some Real Samples. *Microchim. Acta* **2006**, *154*, 321−328.
(70) Hahn, C.; Pribyl, E.; Libber, E.; Caldwell, B. P.; Smith, G. B. L. Reduction Potentials of Nitroguanidine Systems 1223 [Contribution from the Department of Chemistry, Polytechnic Institute of Brooklyn] Reduction of Nitroguanidine. XII. Oxidation Potentials of the Nitro-Nitrosoguanidine and the Nitroso-Aminoguanidine Systems1. *J. Am. Chem. Soc.* **1944**, *66*, 1223−1226.
(71) Nowell, L. H.; Moran, P. W.; Schmidt, T. S.; Norman, J. E.; Nakagaki, N.; Shoda, M. E.; Mahler, B. J.; Van Metre, P. C.; Stone, W. W.; Sandstrom, M. W.; et al. Complex Mixtures of Dissolved Pesticides Show Potential Aquatic Toxicity in a Synoptic Study of Midwestern U.S. Streams. *Sci. Total Environ.* **2018**, *613*−*614*, 1469−1488.
(72) Soltani, N.; Oliveira, M. C.; Alves, G. S.; Werle, R.; Norsworthy, J. K.; Sprague, C. L.; Young, B. G.; Reynolds, D. B.; Brown, A.; Sikkema, P. H. Off-Target Movement Assessment of Dicamba in North America. *Weed Technol* **2020**, *34*, 318−330.
(73) Wang, M.; Li, Z. Nano-Composite ZrO2/Au Film Electrode for Voltammetric Detection of Parathion. *Sens. Actuators, B* **2008**, *133*, 607−612.
(74) Parham, H.; Rahbar, N. Square Wave Voltammetric Determination of Methyl Parathion Using ZrO2-Nanoparticles Modified Carbon Paste Electrode. *J. Hazard. Mater.* **2010**, *177*, 1077−1084.
(75) Aghaie, A.; Khanmohammadi, A.; Hajian, A.; Schmid, U.; Bagheri, H. Nonenzymatic Electrochemical Determination of Paraoxon Ethyl in Water and Fruits by Graphene-Based NiFe Bimetallic Phosphosulfide Nanocomposite as a Superior Sensing Layer. *Food Anal. Methods* **2019**, *12*, 1545−1555.
(76) Xu, X.; Guo, Y.; Wang, L.; He, K.; Guo, Y.; Wang, X.; Gunasekaran, S. Hapten-Grafted Programmed Probe as a Corecognition Element for a Competitive Immunosensor to Detect Acetamiprid Residue in Agricultural Products. *J. Agric. Food Chem.* **2018**, *66*, 7815−7821.
(77) Li, G.; Meng, Z.; Qian, J.; Ho, C.-L.; Lau, S. P.; Wong, W.-Y.; Yan, F. Inkjet Printed Pseudocapacitive Electrodes on Laser-Induced Graphene for Electrochemical Energy Storage. *Mater. Today Energy* **2019**, *12*, 155−160.
(78) Ma, W.; Zhu, J.; Wang, Z.; Song, W.; Cao, G. Recent Advances in Preparation and Application of Laser-Induced Graphene in Energy Storage Devices. *Mater. Today Energy* **2020**, *18*, No. 100569.
(79) Conway, B. E. Transition from "Supercapacitor" to "Battery" Behavior in Electrochemical Energy Storage. *J. Electrochem. Soc.* **1991**, *138*, 1539−1548.
(80) Liu, Z.; Yuan, X.; Zhang, S.; Wang, J.; Huang, Q.; Yu, N.; Zhu, Y.; Fu, L.; Wang, F.; Chen, Y.; et al. Three-Dimensional Ordered Porous Electrode Materials for Electrochemical Energy Storage. *NPG Asia Mater.* **2019**, *11*, No. 12.
(81) Torrente-Rodríguez, R. M.; Tu, J.; Yang, Y.; Min, J.; Wang, M.; Song, Y.; Yu, Y.; Xu, C.; Ye, C.; IsHak, W. W.; et al. Investigation of Cortisol Dynamics in Human Sweat Using a Graphene-Based Wireless mHealth System. *Matter* **2020**, *2*, 921−937.
(82) Torrente-Rodríguez, R. M.; Lukas, H.; Tu, J.; Min, J.; Yang, Y.; Xu, C.; Rossiter, H. B.; Gao, W. SARS-CoV-2 RapidPlex: A Graphene-Based Multiplexed Telemedicine Platform for Rapid and Low-Cost COVID-19 Diagnosis and Monitoring. *Matter* **2020**, *3*, 1981−1998.

https://doi.org/10.1021/acssensors.1c01082
ACS Sens. 2021, 6, 3063−3071